Network Survivability in User-Centric Distributed Massive MIMO with Segmented Fronthaul: Centralized and Distributed Indoor Processing

Jorge G. S. Costa, Yasmim K. C. Costa, André L. P. Fernandes,
André M. Cavalcante and João C. W. A. Costa

***Abstract*— This work investigates hardware failure compensation in a segmented fronthaul structure, operating under the User-Centric (UC) distributed massive MIMO (D-mMIMO) communication paradigm, also referred to as cell-free massive MIMO. The study evaluates the effects of failures, protection schemes, performance degradation, and operational costs across different user densities, taking into account serial fronthaul connections with limited capacity and dynamic bit allocation. Findings highlight that in most configurations, a cross-connection (CC) failure compensation outperforms alternatives involving duplication, offering the best balance between reliability and cost in centralized and distributed processing, benefiting particularly from the latter.**

***Keywords*— Segmented fronthaul, Failure compensation, User-Centric, Cell-free massive MIMO, Protection schemes, Operational costs.**

I. Introduction

User-centric (UC) distributed massive MIMO (D-mMIMO), also referred to as cell-free (CF) massive MIMO, represents a high-density wireless network architecture in which a large number of distributed transmission and reception points (TRPs) cooperatively transmit and receive users' equipment (UEs) signals in a coordinated fashion. This type of network is recognized as a promising solution for 6G, since it can increase spectral efficiency (SE) and provide consistent service coverage. The signal processing in UC D-mMIMO can be centralized or distributed. In the first case, central processing units (CPUs) perform channel estimation and combining/precoding processing steps. In the second case, these steps are carried out on the TRPs. In both cases, CPUs handle baseband processing and overall coordination using fronthaul connections that link the TRPs to them [1][2].

The deployment of UC D-mMIMO remains a challenging issue in the literature. An approach to simplify this process is fronthaul segmentation, which enhances scalability through a compute-and-forward architecture, where fronthaul links connect multiple TRPs to a central processing unit (CPU) in a serial manner [3][4]. Despite its benefits, this configuration may raise reliability concerns. For example, certain failures could disconnect multiple TRPs at once, leading to significant performance degradation. To mitigate this, [5] investigates protection mechanisms, including partial duplication, full duplication and cross-connection as viable solutions to enhance system resilience. Complementary to this, [6] investigates the impact of limited-capacity fronthaul links and how cross-connection protection performs under such constraints. The study assesses whether these redundancy schemes remain effective in practical scenarios with bandwidth limitations.

Despite this, the protection schemes evaluated in [5] and [6] did not account for the impact of variable fronthaul bit rates, nor did they consider any cost figures or centralized processing techniques, such as the partial minimum mean square error (PMMSE) precoding. This latter technique is more effective at canceling interference and is possibly the best way to implement UC D-mMIMO networks. Furthermore, the implementation costs of each scheme were not addressed. Considering all these aspects is essential to provide a comprehensive overview of the advantages and disadvantages of each possible protection strategy. This will help mitigate the effects of failures in the segmented fronthaul, which could lead to unexpected performance issues depending on the available resources if left unattended.

In this context, this study investigates the effects of protection schemes under variable fronthaul bit rates and the impact of different types of precoding techniques, while handling failures across the segmented fronthaul during extended operation periods. The study also examines the implementation costs of each scheme to identify the most effective approach in practical scenarios.

II. System model

It is assumed that the downlink operation of a UC D-mMIMO system with a fronthaul network that serially connects the TRPs, as presented in [5]. The system was L TRPs, K users, N antennas per TRP, and S serial buses (SBs). Additionally, the system operates under time division duplex (TDD) mode within a coherence block with τ_c samples, with τ_p orthogonal pilots used for user channel estimation, allowing each TRP to serve up to τ_p UEs.

A correlated ricean channel model is considered as presented in [5], in such a way that there will be a channel $\mathbf{h}_{s,t,k} \in \mathbb{C}^{N\times 1}$ between the TRP t in the SB s to the user k, which can also be represneted as $\mathbf{h}_{l,k}$, as each pair (s,t) is mapped to one TRP $l \in \{1,\cdots,L\}$ in the system.

Jorge G. S. Costa[1], Yasmim K. C. Costa[1], André L. P. Fernandes[1], André M. Cavalcante[2] and João C. W. A. Costa[1]. [1]Applied Electromagnetism Laboratory, Federal University of Pará - UFPA, Belém, Brazil, [2]Ericsson Research, Ericsson Telecomunicações Ltda., Indaiatuba, Brazil. E-mails: jorge.costa@itec.ufpa.br; yasmim.costa@itec.ufpa.br; andrelpf@ufpa.br; andre.mendes.cavalcante@ericsson.com; jweyl@ufpa.br. This work was partially supported by Ericsson Telecomunicações Ltda, CNPq and CAPES.

The achieved rate for the users modeled according to the linear fronthaul data quantization approximation described in [7], in such a way it can be calculated as

$$\mathrm{SE}_k = \left(1 - \frac{\tau_p}{\tau_c}\right) \log_2 \left(1 + \frac{\mathrm{DS}_k}{\mathrm{IS}_k - \mathrm{DS}_k + \mathrm{QN}_k + \sigma^2_{\mathrm{dl}}}\right), \quad (1)$$

where DS_k, IS_k, QN_k and σ^2_{dl} are the powers of the desired signal, interference signals, fronthaul quantization noise power, and additive white gaussian noise, respectively. The values for the first three variables are calculated as

$$\begin{aligned}
\mathrm{DS}_k &= \left| \sum_{l=1}^{L} \alpha_{l,k} \mathbb{E}\left\{ \sqrt{\rho_{l,k}}\, \mathbf{h}^{\mathrm{H}}_{l,k} \mathbf{D}_{l,k} \overline{\mathbf{w}}_{l,k} \right\} \right|^2, \\
\mathrm{IS}_k &= \sum_{i=1}^{K} \mathbb{E}\left\{ \left| \sum_{l=1}^{L} \alpha_{l,k} \sqrt{\rho_{l,i}}\, \mathbf{h}^{\mathrm{H}}_{l,k} \mathbf{D}_{l,i} \overline{\mathbf{w}}_{l,i} \right|^2 \right\}, \\
\mathrm{QN}_k &= \begin{cases} \mathbb{E}\left\{ \left| \sum_{l=1}^{L} \mathbf{h}^{\mathrm{H}}_{l,k} \mathbf{D}_{l,i} \mathbf{q}_l \right|^2 \right\}, \text{for Cent. P.} \\ \mathbb{E}\left\{ \left| \sum_{l=1}^{L} \mathbf{h}^{\mathrm{H}}_{l,k} \mathbf{D}_{l,i} \sum_{i=1}^{K} \overline{\mathbf{w}}_{l,i} q_{l,i} \right|^2 \right\}, \text{for Dist. P.} \end{cases},
\end{aligned} \quad (2)$$

where $\rho_{l,k}$ is the downlink power from TRP l to user k, $\mathbf{D}_{l,k}$ is the service diagonal matrix constructed from the set $\mathcal{D}_l$, which is the set of users served by TRP l. In summary, $\mathbf{D}_{l,k}$ is $\mathbf{I}_N$ if $k \in \mathcal{D}l$ and $\mathbf{0}_N$ otherwise. The variable $\alpha_{l,k}$ is the quantization distortion factor between TRP l and UE k. In centralized processing implementation, $\alpha_{l,k} = \alpha_l$, indicating that distortion occurs only at the TRP level. Additionally, the variable $\overline{\mathbf{w}}_{l,k} \in \mathbb{C}^{N \times 1}$ represents the unit-power precoding vector for the channel between TRP l and UE k. Finally, $\mathbf{q}_l \sim \mathcal{CN}\big(0, \alpha_l (\alpha_l - 1) \sum_{k=1}^{K} \rho_{l,k} \mathbb{E}\{\overline{\mathbf{w}}_{l,k} \overline{\mathbf{w}}^{\mathrm{H}}_{l,k}\}\big)$ denotes the additive quantization noise in the antenna signals for TRP l in a centralized processing implementation, and $q_{l,i} \sim \mathcal{CN}\left(0, \alpha_{l,i} (\alpha_{l,i} - 1) \rho_{l,i}\right)$ represents the additive quantization noise for the signal of UE i on TRP l in a distributed processing implementation [1][8].

A. Fronthaul Bit Allocation and Bitrate

Two bit-allocation algorithms for fronthaul transmissions are considered: one for distributed processing and another for centralized processing, which are described in Algorithms 1 and 2 of [8], respectively. Both algorithms determine the bit allocation for quantized data samples based on a maximum acceptable SE degradation (a_{deg}), ensuring fronthaul quantization stays within this limit for the worst-case UE. The distributed processing algorithm outputs an array of bit allocations for each user's data stream ($b^{\mathrm{data}}_{l,k}$) across all L TRPs. In contrast, the centralized method provides a scalar bit allocation value (b^{data}_{l}) applicable globally to all TRPs.

Based on that, the fronthaul bitrate for an TRP t in a SB s for distributed processing can be obtained as

$$F_{s,t} = 2B \left(1 - \frac{\tau_p}{\tau_c}\right) \sum_{k \in \mathcal{D}_{s,\to t}} b^{\mathrm{data}}_{l,k}, \quad (3)$$

where B is the total available bandwidth and $\mathcal{D}_{s,\to t}$ represents the set of users that an TRP t and the ones after it in the chain of connections will serve in a SB s, which can be obtained by the union of the $\mathcal{D}_l$ of these TRPs, because each TRP l is mapped to a pair (s,t). For centralized processing the fronthaul bitrate for an TRP t in a SB s is

$$F_{s,t} = \sum_{t'=t}^{M_s} 2NB \left[\left(1 - \frac{\tau_p}{\tau_c}\right) b^{\mathrm{data}}_{l} + \frac{\tau_p}{\tau_c} b^{\mathrm{pil}}_{l} \right], \quad (4)$$

where N is the number of antennas per TRP, M_s is the number of TRPs in the serial bus s, and b^{pil}_{l} is amount of bits used to represent pilot samples.

III. Cost Model

This section presents the Total Cost of Ownership (TCO) model used for the analysis of network implementation with segmented fronthaul for indoor environments. The TCO normalized per the expected user rate is given by:

$$\boldsymbol{TCO} = \frac{\boldsymbol{CAPEX + OPEX}}{\boldsymbol{R_k}}, \quad (5)$$

where CAPEX is the network installation cost, OPEX is the operational costs [9] and $\boldsymbol{R_k} = \boldsymbol{B} \cdot \mathrm{SE}_{\boldsymbol{k}}$ is the expected user rate under cumulative failures. The CAPEX calculation is determined by:

$$\boldsymbol{CAPEX} = \boldsymbol{C^{Indoor}_{cab}} + \boldsymbol{C^{Eq}_{Pur}} + \boldsymbol{C^{Eq}_{Inst}}, \quad (6)$$

where $\boldsymbol{C^{Indoor}_{cab}}$ is the cost of the indoor cabling, $\boldsymbol{C^{Eq}_{Pur}}$ is the purchase cost of the equipment and $\boldsymbol{C^{Eq}_{Inst}}$ is the installation cost of the equipment. The cost of indoor cabling ($\boldsymbol{C^{Indoor}_{cab}}$) is given by:

$$\boldsymbol{C^{Indoor}_{cab}} = \sum_{\boldsymbol{c} \in \boldsymbol{\mathcal{C}}} \boldsymbol{L^{Fiber}_{Indoor,c}} \cdot \boldsymbol{Pr^{Fiber}_{Indoor,c}}, \quad (7)$$

where $\boldsymbol{\mathcal{C}}$ is the set of fibers with different capacity that can be adopted, $\boldsymbol{L^{Fiber}_{Indoor,c}}$ is the length of fiber cables with capacity $\boldsymbol{c}$ and $\boldsymbol{Pr^{Fiber}_{Indoor,c}}$ is the cost of fiber cables with capacity $\boldsymbol{c}$. The purchase cost of the equipment ($\boldsymbol{C^{Eq}_{Pur}}$) is expressed by:

$$\boldsymbol{C^{Eq}_{Pur}} = \sum_{\boldsymbol{i}} \boldsymbol{N^{Eq}_i} \cdot \boldsymbol{Pr^{Eq}_i}, \quad (8)$$

where the $\boldsymbol{i}$ index represents the types of equipment present in the scenario, $\boldsymbol{N^{Eq}_i}$ and $\boldsymbol{Pr^{Eq}_i}$ are the number of equipments of type $\boldsymbol{i}$ and the purchase price of equipment $\boldsymbol{i}$, respectively. The purchase cost of the equipment ($\boldsymbol{C^{Eq}_{Inst}}$) is determined by:

$$\boldsymbol{C^{Eq}_{Inst}} = \sum_{\boldsymbol{j}} [(\boldsymbol{T^{Eq}_j} \cdot \boldsymbol{Sal}) + \boldsymbol{V}], \quad (9)$$

where the $\boldsymbol{j}$ index represents the types of equipment, $\boldsymbol{T^{Eq}_j}$ is the time installation of the equipment $\boldsymbol{j}$ in hours, $\boldsymbol{Sal}$ are the salaries of the working teams, $\boldsymbol{V}$ is the cost of dislocation to install the equipment in hours, that is assumed by:

$$\boldsymbol{V} = \left\lceil \sum_{\boldsymbol{j}} \frac{\boldsymbol{T^{Eq}_j}}{(\boldsymbol{T^{day}} - \boldsymbol{T_d})} \right\rceil \cdot \boldsymbol{T_d}, \quad (10)$$

where T^{day} is the daily working time and T_d is the expected travel duration in hours.

The OPEX calculation is given by:

$$OPEX = C_{Rp} + C_{Ene}, \tag{11}$$

where C_{Rp} and C_{Ene} are the costs for repairs and electric power consumption, respectively. In addition, the cost for repairs (C_{Rp}) is calculated by the equation:

$$C_{Rp} = \left(T_d + \sum_i \left(\frac{N_i}{MTBF_i} \right) \cdot T_{ope} \cdot T_{rep,i} \right) \cdot Sal, \tag{12}$$

where the i also represents the different types of equipment, $MTBF_i$ is the mean time between failures of each type of devices, T_{ope} is the time of operation in hours and $T_{rep,i}$ is the time of reparation of each equipment. To conclude, the cost for electric power consumption (C_{Ene}) is determined by:

$$C_{Ene} = (T_{ope} - T_{fail}) \cdot \sum_i Co_i \cdot Pr_{kwh}, \tag{13}$$

where the i still represents the different types of equipment, T_{fail} is the time of fail in hours, Co_i is the comsuption power of each equipment and Pr_{kwh} is the price of 1 kilowatt hour.

IV. Numerical Results

A. Case Study

This study investigates a fronthaul-constrained UC D-mMIMO system covering an area of 100 m × 100 m with 24 TRPs spaced 20 meters between themselves across the walls of the scenario, as represented in Fig 1.

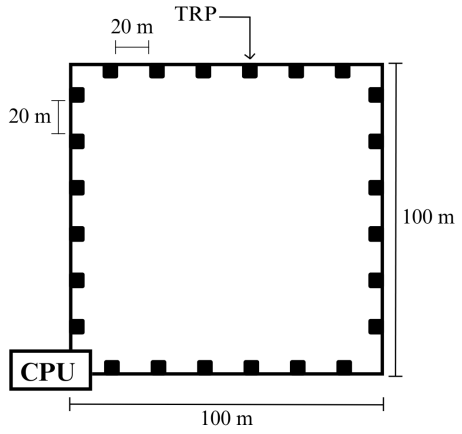

Fig. 1. Illustration of the simulated scenario

The TRPs can be serially connected in six different ways. The first configuration has one SB with 24 TRPs, the second has two SBs, each with 12 TRPs, and this goes on until 6 SBs, each with 4 TRPs. In all cases, the number of antennas per TRP was fixed at $N = 4$ and optical fibers are used to connect the TRPs.

To capture different load conditions, all scenarios are evaluated with 8, 16, and 24 UEs, representing non-crowded, intermediate, and crowded scenarios. The heights of the UE and TRP are set to 1.65 m and 5 m, respectively. The local partial minimum mean square error (LPMMSE) and PMMSE precoding schemes are considered to represent centralized and distributed processing approaches, respectively. Besides that, the other radio parameters are the same as the ones in [5].

For the failure simulations, four cases are considered: (i) No Protection (NP), (ii) Full Duplication (FD), (iii) Partial Duplication (PD), and (iv) Cross-Connection (CC). NP represents a network without any protection scheme. In FD, fronthaul SBs are fully duplicated, whereas PD duplicates up to 40% of the SBs length. CC, on the other hand, establishes cross-connections between fronthaul SBs. The process of failure simulations follow a Markov Chain Monte Carlo Failure Modeling as the outlined on [5].

TABLE I
Cost Parameters

Equipment	Cost (CU)	Inst. Time (min)	Power Consump. (W)	MTBF (h)
TRP	1	4	15	5.2×10^5
Optical Fiber ($> 10\ Gbps$)	0.02/m	-	0	10^8
Optical Fiber ($\leq 10\ Gbps$)	0.008/m	-	0	10^8
Optical switch or key	0.16	10	0	5×10^6
Small Form-factor Pluggable	-	-	0	2.3×10^6

Finally, Table I presents the relevant installation, power, failure and cost parameters for each type of equipment in the network, [5][10]. Notably, the TRP price is equal to one, because it is this work cost unit (CU). The cost of fiber per meter is estimated based on the values contained in [10][11]. Furthermore, the daily working time, the salaries for the working teams and the price of kilowatt hour are defined as 8 h, 0.63 CU/h and 3.33×10^{-5} respectively [10].

B. Degradation Results

Figs 2, 3, and 4 illustrate the degradation levels of network spectral efficiency (SE) over five years of operation under multiple failure conditions, assuming no repairs are performed during this period and self-compensation occurs, considering different user densities: 8, 16, and 24 users, respectively. In all scenarios, degradation decreases as the number of SBs increases, showing the positive effect of segmentation on network robustness. Protection schemes consistently outperform the unprotected baseline, and the FD scheme stands out as the most effective across all cases. It maintains degradation levels below 10%, 15%, and 20% in the 8, 16, and 24 user cases, respectively, due to its high fault tolerance from full equipment redundancy. While FD offers the best performance, it is resource-intensive, motivating the consideration of other alternatives. Among these, the PD scheme proves to be the most beneficial up to a four-SB configuration. Beyond that

point, the CC scheme becomes more advantageous, often achieving degradation results close to those of FD, especially in highly segmented networks.

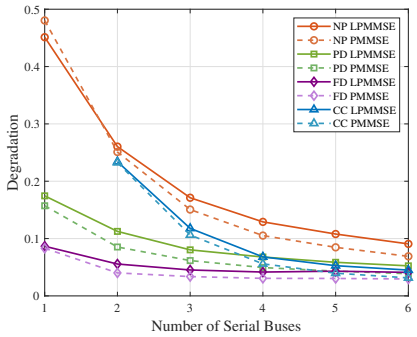

Fig. 2. Degradation in five years of operation with each protection scheme for 8 users

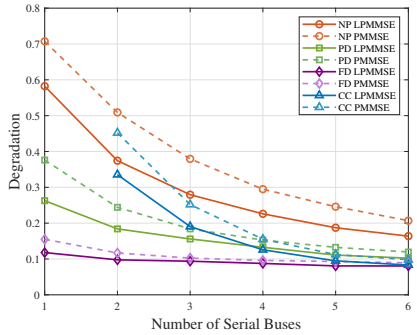

Fig. 3. Degradation in five years of operation with each protection scheme for 16 users

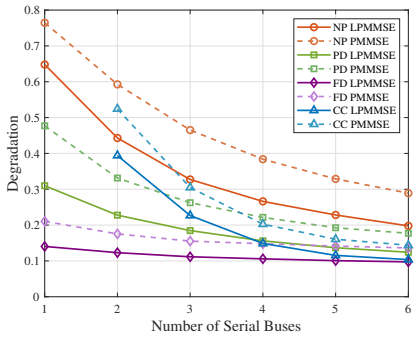

Fig. 4. Degradation in five years of operation with each protection scheme for 24 users

Processing strategy also plays a key role in performance. With 8 users, centralized processing performs better than distributed processing, which aligns with the expected behavior of centralized precoding in scenarios with low user density. However, as the number of users increases to 16 and 24, this trend reverses, and distributed processing becomes more effective. This change reflects the scalability advantage of distributed architectures under heavier loads. The impact of increased user count is also evident in the degradation values observed without protection: from just under 50% in the 8 users case to over 70% and around 78% for 16 and 24 users, respectively. Although the jump in degradation is more pronounced from 8 to 16 users, the 24 users case still shows a moderate but relevant increase, emphasizing how crowded scenarios impose additional stress on the network. Despite this, the consistent pattern across figures confirms that segmentation and suitable protection schemes, especially FD and CC, can mitigate performance loss effectively. This highlights the importance of carefully selecting both the processing strategy and protection mechanism to maintain network efficiency under evolving operational demands.

C. Cost Results

Figs 5, 6 and 7 present the TCO over five years of operation under the same conditions described for the previous graphs, under different protection schemes and user densities (8, 16, and 24 UEs, respectively), normalized by the users SE achieved by the users during this period and considering both centralized and distributed processing.

For 8 users, the lowest TCO appears in the CC scheme, ranging from approximately 5 CU with centralized processing to 10 CU with distributed processing, particularly in the case with three SBs. In contrast, the FD scheme reaches up to 6 CU and 12 CU in centralized and distributed processing respectively, being these the highest TCO for this configuration of users. As the number of users increases, degradation intensifies, raising costs in all schemes. With 16 users, the lowest cost is again found in the CC scheme with four segments, reaching around 10 CU in centralized processing and 23 CU in the distributed. Conversely, FD reach the highest TCO again, being the peaks at 19 CU (centralized) and 45 CU (distributed). For 24 users, CC maintains the best performance with 20 CU and 32 CU in centralized and distributed processing respectively, whereas FD reaches 31 CU and 51 CU under the same conditions still maintaing the CC as the lowest TCO and FD as de highest. These results confirm that the cost advantage of CC becomes more prominent as user count increases, while FD becomes increasingly costly.

In general, the results exhibits a concave behavior on all the curves, with most types of protection schemes reaching their minimum at two SBs for both processing configurations. However, some cases, such as the CC protection one, may reach their minimum at three or even four SBs, depending on whether the processing is centralized or distributed. The CC protection scheme consistently yields the lowest TCO across all user loads and segmentation levels, especially between two and four segments. The FD scheme, on the other hand, is the most expensive due to its need for duplicated equipment, regardless of the SBs. Distributed processing, although more costly, proves to be more robust and scalable in the deployments. For high user counts, distributed CC not only offers the lowest costs among all protection schemes but also demonstrates significantly lower sensitivity to degradation compared to centralized FD. In the 24 users scenario, for example, distributed CC with four SBs costs around 32 CU, an amount close to that of centralized FD. In contrast, distributed

FD exceeds 50 CU, showing a difference of nearly 20 CU when compared to distributed CC, being them under the same processing approach. Even with six SBs, CC remains more cost-efficient than FD under all configurations. These findings highlight that distributed CC is the most cost-effective and resilient option for long-term protection, especially in high-density user environments, while FD should be avoided in such contexts due to its significantly higher costs.

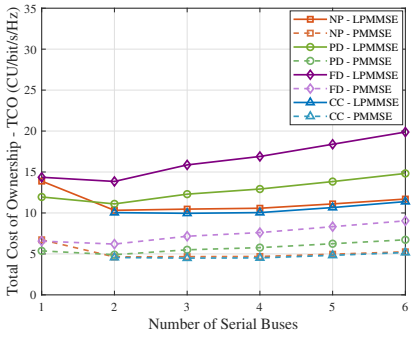

Fig. 5. Total Cost Ownership (TCO) over five years for the scenario with 8 users.

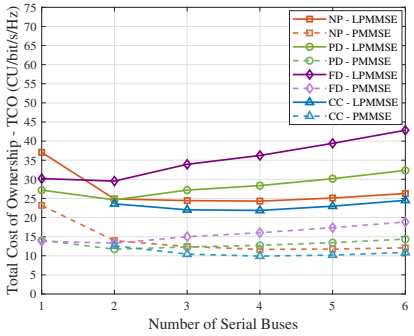

Fig. 6. Total Cost Ownership (TCO) over five years for the scenario with 16 users.

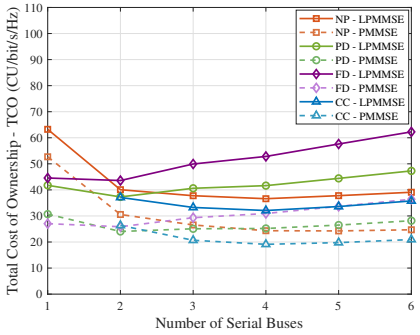

Fig. 7. Total Cost Ownership (TCO) over five years for the scenario with 24 users.

V. Conclusions

This paper investigated hardware failure compensation methods for UC-DmMIMO with segmented fronthaul connections, considering a system with limited fronthaul capacity using a dynamic bit allocation that mitigates noise quantization effects in indoor environments. The results showed that lower segmentation levels (fewer TRPs connected serially) significantly reduced performance degradation due to failures across all user densities. Centralized processing exhibited lower user rate degradation due to failures under low user densities, whereas distributed processing showed lower user rate degradation in other cases. Among protection schemes, FD achieved the lowest degradation, but with a high TCO. Conversely, the CC scheme emerged as the most cost-effective, especially between two and four SBs are present, delivering near FD performance at significantly lower cost, making it the preferred choice for reliable and efficient UC-DmMIMO deployments. Future works can expand the presented analysis for outdoor deployments and use wireless protection schemes

VI. Acknowledgments

The authors would like to thank the High Performance Computing Center (CCAD) of Federal University of Pará (UFPA) for providing the computational resources essential for the simulations in this work.

References

[1] Ö. Demir, E. Björnson, and Sanguinetti, *Foundations of User-Centric Cell-Free Massive MIMO.* Foundations and Trends® in Signal Processing, 2021, vol. 14, no. 3-4.

[2] H. Q. Ngo, G. Interdonato, E. G. Larsson, G. Caire, J. G. Andrews, "Ultradense Cell-Free Massive MIMO for 6G: Technical Overview and Open Questions", *Proceedings of the IEEE*, vol. 112, no. 7, pp. 805–831, July 2024.

[3] V. Ranjbar, R. Beerten, M. Moonen, S. Pollin, "Cell-Free Massive MIMO With Sequential Fronthaul Architecture and Limited Memory Access Points", *IEEE Trans. Wireless Commun.*, vol. 72, no. 12, pp. 7611–7626, Dec. 2024.

[4] G. Interdonato, E. Björnson, H. Q. Ngo et al., "Ubiquitous Cell-Free Massive MIMO Communications", *EURASIP J. Wireless Commun.*, vol.2019, no.1, Aug. 2019.

[5] A. L. P. Fernandes, D. D. Souza, D. B. da Costa, A. M. Cavalcante, J. C. W. A. Costa, "Cell-Free Massive MIMO With Segmented Fronthaul: Reliability and Protection Aspects", *IEEE Wireless Commun. Lett.*, vol. 11, no. 8, pp. 1580–1584, Aug. 2022.

[6] J. G. S. Costa, Y. K. C. Costa, J. F. M. Oliveira, A. L. P. Fernandes, A. M. Cavalcante, and J. W. Costa, "Evaluating cross-connection fronthaul redundancy schemes for segmented user-centric distributed massive MIMO under limited capacity links," in *Proc. Braz. Symp. on Telecommun. Signal Process.* (SBrT), 2024.

[7] G. Femenias, F. Riera-Palou, *"Fronthaul-Constrained Cell-Free Massive MIMO With Low Resolution ADCs"*, IEEE Access, vol. 8, pp. 116195–116215, 2020.

[8] A. L. P. Fernandes et al., "A Cost Assessment Methodology for User-Centric Distributed Massive MIMO Architectures", *IEEE Open J. Commun. Soc.*, vol. 5, pp. 3517–3543, 2024.

[9] E. J. Oughton, W. Lehr, "Surveying 5G Techno-Economic Research to Inform the Evaluation of 6G Wireless Technologies", *IEEE Access*, vol. 10, pp. 25237–25257, 2022.

[10] C. Mas Machuca, J. Chen and L. Wosinska, "Cost-Efficient Protection in TDM PONs", *IEEE Commun. Mag.*, vol. 50, no. 8, pp. 110-117, August 2012.

[11] R. Armstrong, "How much is fiber optic cable? Top costs revealed 2024," *AccuTech Communications*, Nov. 8, 2023. [Online]. Available: https://accutechcom.com/how-much-is-fiber-optic-cable/